Proceedings of the XVII ECSMGE-2019
Geotechnical Engineering foundation of the future
ISBN 978-9935-9436-1-3

doi: 10.32075/17ECSMGE-2019-0248

XVII European Conference
ECSMGE 2019
Reykjavik
on Soil Mechanics
and Geotechnical Engineering

Full-scale load testing on long prefabricated concrete piles in the Port of Rotterdam

Essais de chargement in situ de longs pieux en béton préfabriqué au port de Rotterdam

I. Matic MSc.
Witteveen+Bos, Deventer, The Netherlands

R. de Nijs MSc. CEng
Witteveen+Bos, Deventer, The Netherlands

Delft University of Technology, Delft, The Netherlands

M. De Vos civ. eng.
Belgian Building Research Institute, Sint Stevens Woluwe, Belgium

A.A. Roubos MSc.
Port of Rotterdam Authority, Rotterdam, The Netherlands

Delft University of Technology, Delft, The Netherlands

ABSTRACT: In 2017 the Dutch national standardization institute (NEN) released a new version of the National Annex to NEN-EN 1997-1 Eurocode 7, including revised reduced pile base factors. This has a significant impact on the dimensions of pile foundations. Consequently, in situ load tests were considered in the Port of Rotterdam. In this study, full-scale static load tests (SLT) were conducted on four prefabricated concrete piles (36 m long), in order to optimize the design of a new quay wall. The test piles were instrumented with several types of optical fibers along the length, enabling detailed registration of shaft friction and base resistance. Since the optical fibers were already installed at casting, unique insights have been acquired regarding the residual stresses in the piles after hardening. These stresses are commonly not taken into consideration, resulting in underestimation of base capacity in favor of shaft. Since the test piles were loaded after different time periods, the effect of aging was additionally investigated in this study. After the completion of the SLT's, fully instrumented rapid load tests (RLT) were conducted on the same four piles. Subsequently, this provided the opportunity to compare and correlate the results of SLT and RLT for different soil types. This paper presents the results, conclusions and recommendations that follow from these tests. The results of this study have been used to optimize the design of the quay wall by reducing the number of piles by approximately 25% and hence, the overall construction costs by 5%.

RÉSUMÉ: En 2017, l'institut national de normalisation néerlandais (NEN) a publié une nouvelle version de l'annexe nationale de la norme NEN-EN 1997-1 Eurocode 7, qui inclut une réduction des facteurs d'installation pour la base du pieu. Cela a un impact significatif sur le dimensionnement des fondations sur pieux. Par conséquent, des essais de chargement in situ ont été envisagés au port de Rotterdam. Dans cette étude, des essais de chargement statique (SLT) à grande échelle ont été réalisés sur quatre pieux en béton préfabriqués (36 m de long), afin d'optimiser la conception d'un nouveau mur de quai. Les pieux de test ont été instrumentés avec plusieurs types de fibres optiques sur la longueur, permettant un enregistrement détaillé du frottement et de la résistance à la base. Les fibres optiques ayant été installées lors de la fabrication des pieux, des connaissances uniques ont été acquises concernant les contraintes résiduelles dans les pieux après l'installation de ceux-ci. Ces contraintes ne sont généralement pas prises en compte, ce qui entraîne une sous-estimation de la résistance à la base en faveur du frottement. Comme les pieux de test ont été chargés après différentes périodes, l'effet du vieillissement a également été étudié dans cette étude. Une fois les tests terminés, des tests de chargement rapide (RLT) entièrement instrumentés ont été effectués sur les quatre mêmes pieux. Par la suite, cela a permis de comparer et de corréler les résultats des SLT et des RLT pour différents types de sol. Ce document présente les résultats, les conclusions et les recommandations découlant de ces tests. Les résultats de cette étude ont été utilisés pour optimiser la conception du mur de quai en réduisant le nombre de pieux d'environ 25% et, en conséquence, les coûts de construction globaux de 5%.

Keywords: Full-scaled load testing; Optical fibers; Rapid load testing; Pile aging; Static load testing

1 INTRODUCTION

Since 2017, a revision of design code NEN-EN1997 became effective, including the obligatory implementation of lower parameter values for α_p, which are significantly influencing the capacity and hence will lead to longer and more robust foundation piles. However, in practice the existing pile foundations, which have mostly not been tested, do not show damage and are performing fairly well. Consequently, it has become necessary to perform in situ load testing in order to optimize the pile dimensions or to comply with the new design regulations and accept higher construction costs. The Port of Rotterdam Authority therefore decided to conduct full-scale static load tests (SLT) on prefabricated concrete piles prior to the construction stage of a project in order to determine the effective capacity and to optimize the pile dimensions required for the design of a new quay wall. In these tests the piles were equipped with new optical fibers along the total length, enabling detailed registration of both shaft friction and base resistance.

2 SOIL INVESTIGATION

Prior to the load tests several cone penetration tests (CPT) have been made to determine geotechnical properties of the soil at the test location in the Port of Rotterdam. Figure 1 shows a typical CPT. The red dashed line represents the installation depth of the test piles.

3 PREPARATION FOR THE TESTS

In order to maximally optimize the design and to comply with NPR7201 (NEN, 2017), it was necessary to test at least 4 prefabricated concrete piles. In order to avoid an extremely high test load, these test piles (measuring 450 x 450 mm) were slightly smaller in cross section than the piles that are actually used in the quay wall, measuring 500 x 500 mm. The test piles were ordered at maximum pre-cast length of 36 m.

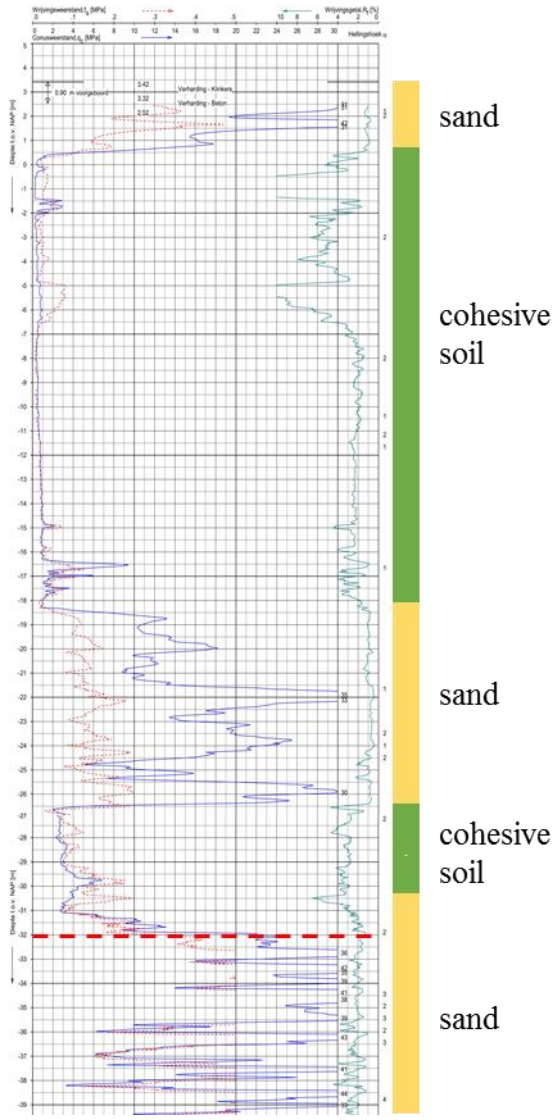

Figure 1. Soil profile at testing site

3.1 Pile bearing capacity

According to the Dutch code NEN-EN 1997 (NEN, 2016), the pile capacity is calculated using the following equations:

$$R_c = R_b + R_s \tag{1}$$

$$R_b = A_b \cdot \frac{1}{2} \cdot \alpha_p \cdot \beta \cdot s \cdot \left(\frac{q_{c;I;gem} + q_{c;II;gem}}{2} + q_{c;III;gem}\right) \quad (2)$$

$$R_s = O_{s;\Delta L;gem} \cdot \int_{\Delta L} \left(\alpha_s \cdot q_{c;z;a}\right) \cdot dz \quad (3)$$

Where:
R_c (kN) is the ultimate pile resistance;
R_b (kN) is the ultimate base resistance;
R_s (kN) is the ultimate shaft resistance;
A_b (m^2) is the pile base surface;
α_p (-) is the pile base factor;
β (-) is the pile toe factor;
s (-) is the pile shape factor;
q_c (MPa) is the measured cone resistance;
O_s (m) is the pile circumference;
α_s (-) is the pile shaft factor;

In order to optimize the design, the pile base factor (α_p) and pile shaft factor (α_s) can be modified on the basis of in situ test results.

Table 1 presents the parameters used for calculating the bearing capacity of the piles, according to the Dutch code for pile testing, NPR7201 (NEN, 2017). The ultimate total, base and shaft resistance is determined for each CPT separately, and only the average values of all CPT's combined are shown in Table 1.

Table 1. Parameters used in (2) and (3)

Parameter	Unit	Value
$\boldsymbol{A_b}$	m^2	0,20
$\boldsymbol{\alpha_p}$ *	-	1,00
$\boldsymbol{\beta}$	-	1,00
$\boldsymbol{s}$	-	1,00
$\boldsymbol{O_s}$	m	1,80
$\boldsymbol{\alpha_s}$	-	0,01
$\boldsymbol{R_b}$	kN	2546
$\boldsymbol{R_s}$	kN	3868
$\boldsymbol{R_c}$	kN	6414

*) according to the norm NEN-EN1997 (2012)

3.2 Testing frame

An appropriate steel test frame was chosen based on the bearing capacity of the piles, using the old Dutch code NEN-EN1997 (NEN, 2012) in order to determine an upperlimit testvalue. The steel test frame was designed to withstand at least 1,5 times the precalculated capacity of the piles. Consequently, two crossed, steel tubes (Ø 1420 mm) were used (Figure 2). The test frame was anchored by eight anchor piles (Ø 82,5 x 20,0 mm), each 45 m long, in order to provide the reaction force for the load tests.

Figure 2. Test frame at location

3.3 Instrumentation of the pile

All four test piles were equipped with optical fibres. Two types of optical fibres were used: Fibre Brag Grating (FBG) and Brillouin scattering (BOFDA). The optical fibres were attached to one of the reinforcement bars along the whole length of the prefabricated concrete piles (prior to pouring the concrete). In addition, temperature sensors were placed in the pile for T-compensation, and a spare tube was installed, should the fibres be damaged during fabrication or installation of the piles. Figure 3 shows the instrumentation in the pile before pouring concrete.

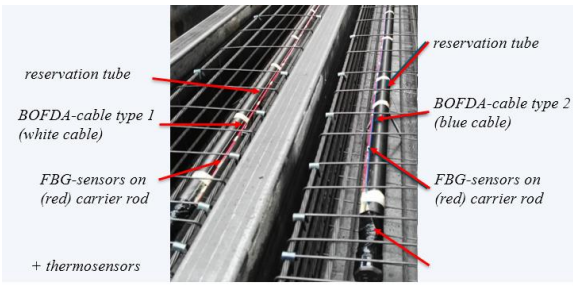

Figure 3. Instrumentation of the pile in formwork

3.4 Testing site instrumentation

During the load tests various aspects were monitored, such as pile head and base displacement, applied load, displacement of the testing frame and anchorrods. Figure 4 and Figure 5 show the monitoring devices used.

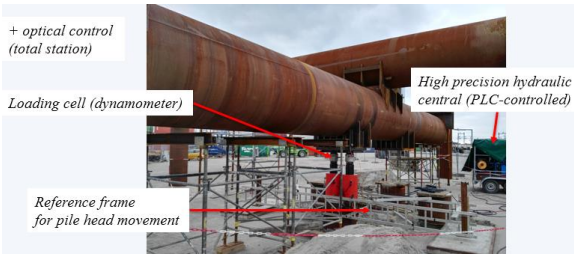

Figure 4. Test site instrumentation 1/2

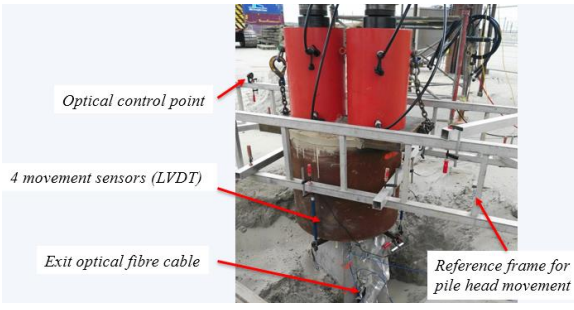

Figure 5. Test site instrumentation 2/2

4 TESTING PROTOCOL

The test protocol was identical for all the piles and was based on NPR7201, class A. Every load step was applied during at least 1 hour, when the creep criterium was satisfied during that hour the next load step could be applied. Otherwise, the load would be held constant until the creep criterium was satisfied, with a maximum of 3 hours per loading step. After each loading step the applied load would be reduced to 200 kN and held for 15 minutes, before applying the next load step. Every new load step would be 500 kN (initial load steps) or 1000 kN higher than the previous one.

The load was increased until significant movement of the pile head was measured, so called pile failure. Failure of the pile was reached at a pile base displacement of 0,1 D_{eq}, which is equal to 50 mm. The loading step before failure was used to determine the ultimate load capacity. After the loading step in which the base displacement was more than 50 mm the test for this pile was ended.

5 INTERPRETING THE SLT RESULTS

5.1 Interpreting the optical fibre readings

During the tests a certain load is applied at the head of the pile. Due to this load the pile starts to move downwards, mobilizing the shaft and base. Depending on the stifness of the pile, a certain elastic shortening occurs along the pile, which was measured with the optical fibers. Now it was possible to translate the deformations in the optical fibers (µstrains) to the corresponding load at that level of the pile, using the following equation:

$$F = \varepsilon \cdot EA \qquad (4)$$

Where:
F (kN) is the corresponding force;
ε (microstrain) is the deformation of the optical fibre;
EA (kN) is the axial stiffness based on Fellenius.

It's crucial to define the correct axial stiffness of the pile, Figure 6 shows an example of defining the strain-based axial stiffness EA, according to Fellenius (Fellenius, 2001).

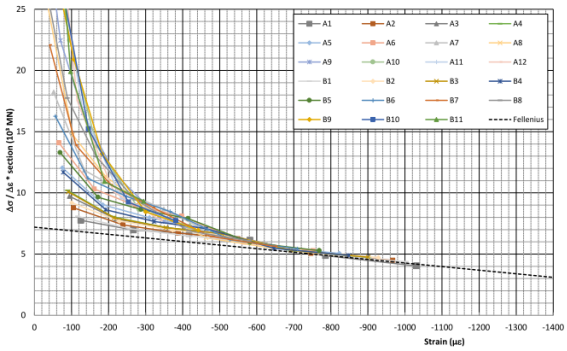

Figure 6. EA according to Fellenius for SLT 2

Using the strain-based EA and the measured strains along the pile, the associated force distribution was generated (Figure 7).

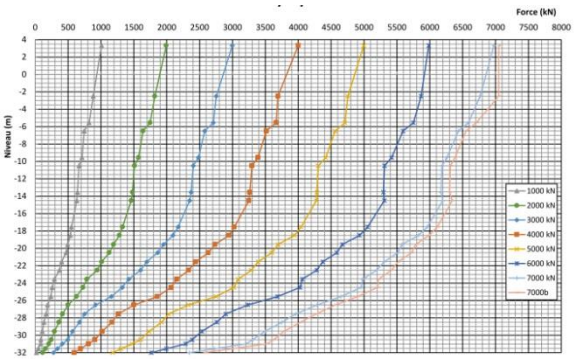

Figure 7. Force distribution along the pile for SLT 2

5.2 SLT results

Table 2 lists the results of the 4 SLT's. The distribution between shaft and base capacity is determined on the basis of the readings from the optical fibres.

Table 2. Results of the SLT's

SLT	R_b (kN)	R_s (kN)	R_c (kN)
SLT1	>2100*	>3900*	>6000*
SLT2	2000	4400	6400
SLT3	2350	4150	6500
SLT4	1600**	5150**	6750**

*) SLT1 was not carried out till ultimate loading, the presented values correspond to a base displacement of 16 mm.

**) In SLT4 the distribution of shaft and base capacity doesn't correlate with the first 3 tests, however, the total capacity does.

As can be seen in Table 2, the results of the first 3 SLT's give a similar distribution of shaft and base capacity, where the fourth SLT does not. However, the total capacity (R_s) of the fourth test pile corresponds with the total. The current explanation for this phenomena is that the interpretation of the so-called residual stresses of the optical fibres after pile installation was more complex at SLT4 and introduced new uncertainties. The measurements of the residual stresses were not straightforward, probably due to the influence of bending moments in the pile during the reference measurements and temperature changes during pile installation. Consequently, the decision was made not to take the results of the fourth (and highest) SLT into consideration for the final design of the quay wall. The load-settlement curves of the first 3 SLT's are shown in Figure 8.

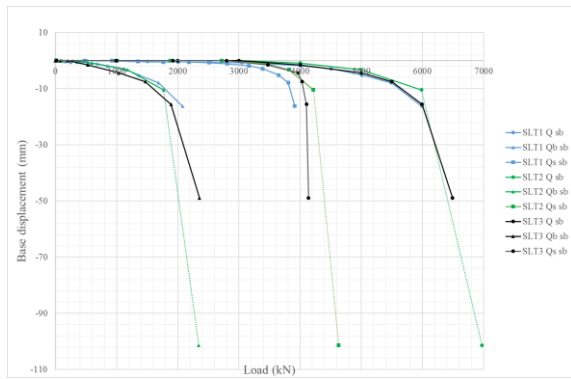

Figure 8. Load-settlement graph SLT

5.3 Effect of the SLT's on the design

Using the results from the first 3 SLT's a new pile base factor (α_p) was calculated, by defining the ratio between the average base resistance from the SLT's and the base resistance using equation (2). The α_p found was equal to this ratio (Table 3).

Table 3. Pile base factor (α_p)

Pile base factor	Symbol	Value
According to 2017 norm	α_p^{2017}	0,70
Based on the SLT's	α_p^{SLT}	0,84

Based on the SLT's the pile base factor was increased by 20%.

Since a significant part of the piles' length does not contribute to the shaft bearing capacity, due to negative skin friction (in the clay layers), the design was optimized by decreasing the number of piles rather than reducing their length. The pile shaft factor (α_s) was not optimized for the same reason. As a result approximately 25% less piles were needed for this quay wall. Hence the total costs of the project were reduced with 5%.

6 PILE AGING

Various studies show that the axial capacity of driven piles in sand increases in the period after insatlation of the pile (a.o. Gavin et al., 2015). To research this effect of aging, the individual pile tests were performed at 1 day, 10 days, 30 days, and approximately 100 days after pile driving. As a result, this timeframe allowed the identification of potential aging effects on pile capacity.

In order to determine that aging has occurred, the measured shaft capacity R_s of each SLT should be higher than the previous one. However, Table 2 shows that this was not the case, because the measured shaft capacity at SLT3 was lower than the one measured by SLT2.

The absence of the effect of aging can probably be explained by the ratio between pile length (L) and pile diameter (D), which equals $L/D \approx 80$ (see also Figure 9). This hypothesis has, however, not yet been confirmed.

7 RAPID LOAD TESTING

After finishing the 4 SLT's, a series of Rapid Load Tests (RLT's) has been performed on the same piles. The type of RLT's executed was StatRapid testing (STR), where a certain mass falls from a certain height on a spring system. After bouncing up from the springs, a catch mechanism catches the drop mass. This prevents unwanted rebounds and allows for successive cyclic testing with increasing loads similar to static load cycling testing. Since the RLT's can be performed relatively fast, all 4 piles were tested within 2 working days. A preview of the STR is shown in Figure 10.

Figure 9. Pile before installation showing the slenderness of the pile

To determine the static bearing capacity based on a RLT, a loading rate factor η must be applied on the measured force in order to correct for the loading rate effect: pile and subsoil act stiffer when a load is applied at fast rate. The loading rate factor for sand is usually around η = 0,85-0,90, while in cohesive soils it can be around η = 0,50 or less, depending on material properties. In this case, a large portion of the pile capacity comes from shaft friction in clayey layers, so an overall loading rate factor close(r) to η = 0,50 should be expected.

Figure 11 shows one of the measured load-displacement diagrams, based on an assumed loading rate factor η =0,85. The pile starts to fail in load cycle 5, at measured load approx.10,8 MN. Compared to the SLT result of the same pile (Rs = 6,4 MN) this suggests an overall loading rate factor η = 6,4/10,8 = 0,60 for this combination of soil profile and toe level.

Since a considerable length of the pile shaft is located in cohesive soil, and the base is only approximately 1 m located in sand, this indicates the correction factor for sand does not apply in this case.

At present there are not enough references for determining a reliable correction factor for the RLT correction factor in cohesive soils. Consequently, the information collected with these tests are not used in the final design but can be very helpful in future research.

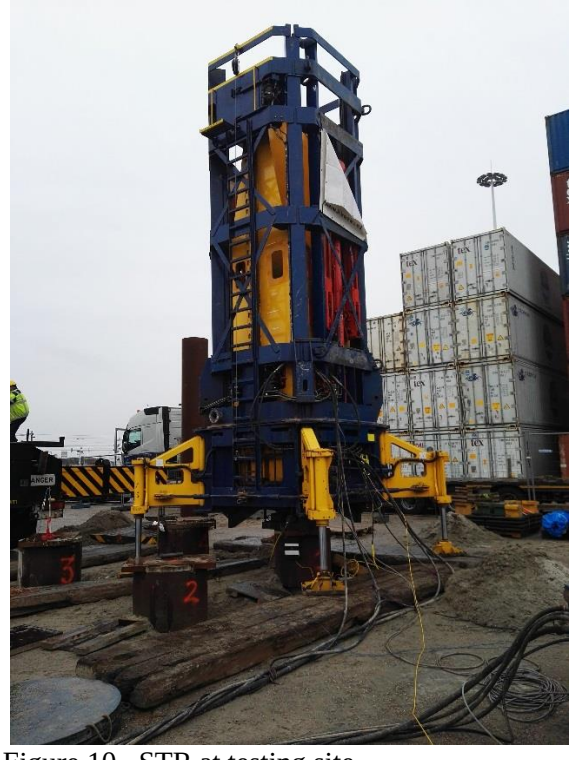

Figure 10. STR at testing site

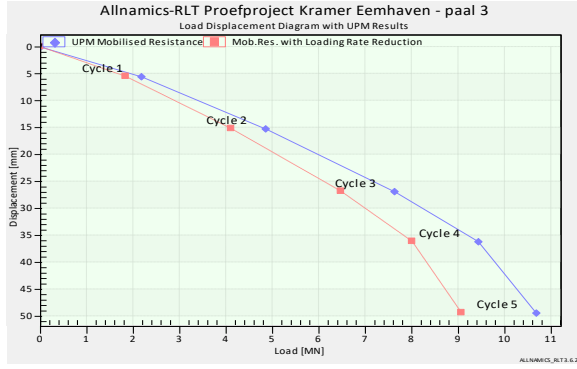

Figure 11. Load-settlement graph RLT at pile P3

8 CONCLUSIONS

The results of this study provided additional understanding of pile behaviour under static and dynamic loading. The most important findings of this study are:

Better understanding in the development of shaft and base resistance. Residual strains after pile installation play an important role in the allocation of shaft and base bearing capacity. Not acknowledging residual strains results in overestimation of the shaft contribution and an underestimation of the base resistance

Total pilebearing capacity was estimated to be within a 10% range over all four SLT's

The measured base resistance of the piles proved to be higher than the calculated base resistance according to NEN-EN1997 (2017). However, it was still lower than the calculated base resistance according to NEN-EN1997 (2012).

The effect of pile aging has not been identified in this study. This could be due to the slenderness of the piles.

Statrapid is a promising technique. Due to circumstances, pile geometry did not provide favorable conditions for statrapid. Shallow penetration in the sand foundation layer made the impact of cohesive soils much bigger and hindered the comparison of Statrapid with SLT.

The total costs of the tests were approximately 320.000 €, while saving approximately 540.000 € on construction costs.

9 ACKNOWLEDGEMENTS

On behalf of the Port of Rotterdam Authority, W+B, BBRI, and TU-Delft the authors whould like to thank all companies and organisations involved for their support, funding and hospitality. In particular, the effort of the contractor DIMCO regarding the installation and practical aspacts and design of the testframe can not be overestimated. Special thanks go to Allnamics, for providing their test apparatus and interpretation of results. The firm also provided detailed insights into the method to asses rapid load tests. Special appreciation goes out to mr. R. Spruit, Gemeente Werken Rotterdam, for reviewing the test procedure and interpretating the results.

10 REFERENCES

Fellenius, B. H., 2001. From Strain Measurements to Load in an Instrumented Pile, Geotechnical News Magazine.

Gavin, K. G., Jardine, R., Karlsrud, K. & Lehane, B. M., 2015. The effects of pile ageing on the shaft capacity of offshore piles in sand, Frontiers in Offshore Geotechnics III, Meyer ed., 129-150, CRC Press/Balkema, Leiden

NEN, 2017, NPR7201 - Geotechnics - Determination of the Axial Bearing Capacity of Foundation Piles by Pile Load Testing, NEN, Delft

NEN, 2012, NEN-EN 1997+C1:2012/NB:2012 - National Annex to NEN-EN 1997-1 Eurocode 7: Geotechnical design - Part 1: General rules, NEN, Delft

NEN, 2016, NEN-EN 19971+C1+A1/NB, 2016 - National Annex to NEN-EN 1997-1 Eurocode 7: Geotechnical design - Part 1: General rules, NEN, Delft

Nijs, R.E.P. de, Kaalberg, F, Osselaer, G, Couck, J, van Royen, K, “Geotechnical monitoring of a trialpit excavation toward the Boom clay in Antwerp (Belgium)”, IGSR, Rotterdam 2015